



## Energy and spin diffusion in the one-dimensional classical Heisenberg spin chain at finite and infinite temperatures

Nianbei Li <sup>\*</sup>

*Institute of Systems Science and Department of Physics, College of Information Science and Engineering, Huaqiao University, Xiamen 361021, China*

 (Received 25 June 2019; revised manuscript received 9 November 2019; published 2 December 2019)

The energy and spin diffusion behaviors in the one-dimensional classical Heisenberg spin chain have been systematically investigated using the equilibrium diffusion method. The spatiotemporal autocorrelation functions for energy and spin are calculated at finite and infinite temperatures. As conserved quantities, the spreading of excess energy and spin can be used to determine their actual diffusion behaviors. At low temperatures, the energy diffusion shows almost ballistic behavior, and spin shows superdiffusion behavior for finite chain size. For energy diffusion, normal diffusion behavior can be obtained when the temperature is higher than 0.75. For spin diffusion, normal diffusion behavior is observed at infinite temperature.

DOI: [10.1103/PhysRevE.100.062104](https://doi.org/10.1103/PhysRevE.100.062104)

### I. INTRODUCTION

As a prototypical model for real magnetic systems, the classical Heisenberg spin chain has been extensively studied both numerically and theoretically. One of the important questions is the actual spin diffusion behavior for the one-dimensional (1D) classical Heisenberg chain at high temperatures. Although the normal diffusive behavior of spin transport is predicted by the phenomenological spin-diffusion theory [1,2], the lack of rigorous microscopic theory leaves space for contradictory claims from numerical simulations [3–10]. In order to numerically explore the spin diffusion behavior, most of the previous studies focus on the dynamics of spin autocorrelation function  $C_s(t) = \sum_i \langle \vec{S}_i(t) \vec{S}_i(0) \rangle / N$  [3–10]. In the asymptotic limit, the power-law time decay of  $C_s(t) \propto t^{-\delta}$  will give the information for spin diffusion behavior. If  $\delta = 1/2$ , the spin diffusion is normal, which is consistent with the prediction from the standard phenomenological spin-diffusion theory. However, if  $\delta > 1/2$ , the spin diffusion behavior is anomalous superdiffusion.

Besides the 1D Fermi-Pasta-Ulam  $\beta$  (FPU- $\beta$ ) lattice and discrete nonlinear Schrödinger equation lattice, the 1D classical Heisenberg spin chain represents another prototypical model for nonlinear systems. The chaotic dynamics is investigated by calculation of the largest Lyapunov exponent at different temperature regimes for an isotropic and ferromagnetic Heisenberg chain [11]. For the past two decades, the study of heat conduction in 1D nonlinear systems has attracted much attention since the discovery of anomalous heat conduction in a 1D FPU- $\beta$  lattice where the thermal conductivity  $\kappa$  diverges with the system size  $N$  as  $\kappa \propto N^\alpha$  with  $\alpha \sim 1/3$ – $1/2$  [12–32]. The diverging thermal conductivities of anomalous heat conduction have been experimentally verified for quasi-1D carbon nanotubes [33,34] and two-dimensional

graphene [35]. The property of heat conduction in a classical Heisenberg chain has also been studied for both ferromagnetic and antiferromagnetic spin chains [36]. Using the equilibrium Green-Kubo method and nonequilibrium molecular dynamics simulation, finite heat conductivities are obtained for the 1D classical Heisenberg spin chain at all values of temperature and external fields [36].

In this paper, we will systematically investigate the energy and spin diffusion behaviors in the 1D classical Heisenberg spin chain at finite and infinite temperatures with the equilibrium diffusion method [37]. For conserved quantities such as energy and momentum in 1D nonlinear atomic lattices, the spatiotemporal autocorrelation functions for excess energy  $C_E(i, t)$  and momentum  $C_P(i, t)$  can be defined and calculated [37]. If the diffusion process is normal, the corresponding distributions  $C_E(i, t)$  or  $C_P(i, t)$  will follow the Gaussian distribution  $\rho_G(i, t) = \frac{1}{\sqrt{4\pi Dt}} e^{-\frac{i^2}{4Dt}}$  where  $D$  is the diffusion constant in the asymptotic time limit. As a result, the mean-square displacement (MSD)  $\langle \Delta x^2(t) \rangle$  of the corresponding conserved quantity will depend on the correlation time in a linear way as  $\langle \Delta x^2(t) \rangle \propto 2Dt^\beta$  with  $\beta = 1$ . There is a connection theory relating energy diffusion to heat conduction via the relation  $\alpha = \beta - 1$  [38]. For normal energy diffusion with  $\beta = 1$ , the corresponding heat conduction is also normal with  $\alpha = 0$ . For ballistic energy diffusion with  $\beta = 2$ , the corresponding heat conduction is ballistic too with  $\alpha = 1$ . However, if the energy diffusion is superdiffusion with  $1 < \beta < 2$ , the corresponding heat conduction is anomalous with  $0 < \alpha < 1$ . The relation between energy diffusion and heat conduction has been numerically verified for 1D nonlinear lattices such as FPU- $\beta$ ,  $\phi^4$ , Frenkel-Kontorova, and coupled rotator models [37–39].

Unlike the nonequilibrium molecular dynamics and equilibrium Green-Kubo methods, the equilibrium diffusion method generates the spatial distribution  $C(i, t)$  over the whole lattice at every correlation time. Once a Gaussian

<sup>\*</sup>nbli@hqu.edu.cn

distribution  $\rho_G(i, t)$  is obtained as  $C(i, t) \sim \rho_G(i, t)$ , the result of normal diffusion can be almost assured. Therefore, in judging the normal diffusion behavior, the equilibrium diffusion method is more advantageous than the traditional nonequilibrium molecular dynamics and equilibrium Green-Kubo methods.

The paper will be organized as follows. In Sec. II the model of the 1D classical isotropic Heisenberg spin chain and the numerical method will be introduced. In Sec. III the energy diffusion behavior at finite and infinite temperatures will be calculated and presented. In Sec. IV the spin diffusion behavior at finite and infinite temperatures will be simulated and discussed. The summary and conclusions will be presented in Sec. V.

## II. MODEL AND METHODS

We study the 1D classical isotropic Heisenberg spin chain with the following Hamiltonian:

$$H = -J \sum_i \vec{S}_i \cdot \vec{S}_{i+1} = \sum_i H_i. \quad (1)$$

The spin chain is ferromagnetic if the interaction strength  $J > 0$ . For simplicity, the interaction strength  $J$  is set as unity and the spin  $\vec{S}_i$  is set as a three-dimensional unit vector. Periodic boundary conditions are also applied with  $\vec{S}_i = \vec{S}_{i+N}$  with  $N$  the total spin sites or the chain length.

The equations of motion can be expressed as

$$\frac{d\vec{S}_i}{dt} = -\vec{S}_i \times \frac{\partial H}{\partial \vec{S}_i} = -\vec{S}_i \times (\vec{S}_{i-1} + \vec{S}_{i+1}). \quad (2)$$

It is straightforward to find that the total energy  $E = \sum_i H_i$  and total spin  $\vec{S} = \sum_i \vec{S}_i$  are conserved. As the current model is isotropic without magnetic field, we can study the diffusion of the  $z$  component of the total spin  $S_z = \sum_i S_{i,z}$  only for simplicity.

In the following numerical calculations we will use the microcanonical simulation with energy density  $e = E/N$  the input parameter. The relation between the energy density  $e$  and the temperature  $T$  can be expressed as [40]

$$e = T - \coth \frac{1}{T}. \quad (3)$$

It is straightforward to obtain that in the low-temperature limit  $T \rightarrow 0$ , the energy density  $e$  approaches to the lowest energy density as  $e \rightarrow -1$ . This lowest energy state corresponds to the state that all the spins  $\vec{S}_i$  are parallel in one direction. In the infinite temperature limit  $T \rightarrow \infty$ , the energy density  $e$  approaches to zero as  $e \rightarrow 0$ . This infinite temperature state represents the state that all spins have totally random directions. The relation between energy density  $e$  and temperature  $T$  of Eq. (3) is plotted in Fig. 1.

The total energy  $E$  is a conserved quantity. To investigate the energy diffusion, the spatiotemporal correlation function of energy fluctuation  $C_E(i, t)$  can be defined as [37]

$$C_E(i, t) = \frac{\langle \Delta H_i(t) \Delta H_0(0) \rangle}{\langle \Delta H_0(0) \Delta H_0(0) \rangle} + \frac{1}{N-1}, \quad (4)$$

where  $H_i = -\vec{S}_i \cdot \vec{S}_{i+1}$  is the local energy for the  $i$ th site and  $\Delta H_i(t) = H_i(t) - \langle H_i(t) \rangle$  denotes the real time local energy

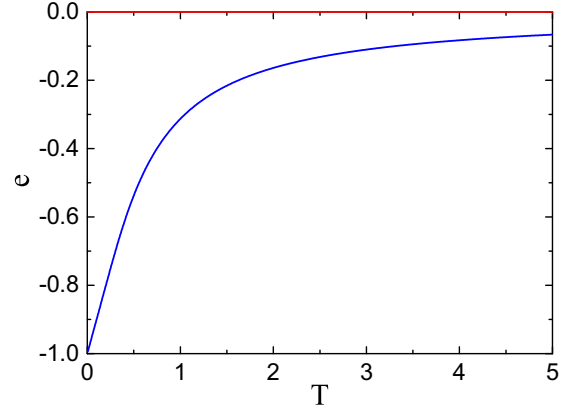


FIG. 1. The relation  $e = T - \coth \frac{1}{T}$  of Eq. (3) between the energy density  $e$  and temperature  $T$  for the isotropic 1D Heisenberg spin chain. The energy density  $e = -1$  corresponds to the zero temperature  $T = 0$  case, and the energy density  $e = 0$  represents the infinite temperature  $T = \infty$  case.

fluctuation. The  $\langle \cdot \rangle$  is the ensemble average which is equivalent to the time average as the system is chaotic and ergodic. For simplicity, the total size  $N$  is chosen as an odd value, and the site index  $i$  will range from  $-(N-1)/2$  to  $(N-1)/2$ . The introduction of the extra term  $1/(N-1)$  is due to the use of a closed system, and energy density instead of temperature is the input parameter. This extra term will vanish in the thermodynamic limit of  $N \rightarrow \infty$ . At the initial correlation time  $t = 0$ , the distribution  $C_E(i, t = 0) = \delta_{i,0}$  is a Kronecker delta function by definition. Therefore, the spatiotemporal distribution  $C_E(i, t)$  describes the spreading of the energy fluctuation across the spin chain. The detailed spatiotemporal behavior of distributions  $C_E(i, t)$  will give the information about energy diffusion for the Heisenberg spin chain.

Since the  $z$  component of total spin  $S_z$  is also conserved, we can define the spatiotemporal correlation function of spin fluctuation  $C_{S_z}(i, t)$  as [37]

$$C_{S_z}(i, t) = \frac{\langle \Delta S_{i,z}(t) \Delta S_{0,z}(0) \rangle}{\langle \Delta S_{0,z}(0) \Delta S_{0,z}(0) \rangle} + \frac{1}{N-1}, \quad (5)$$

where  $\Delta S_{i,z}(t) = S_{i,z}(t) - \langle S_{i,z} \rangle$  represents the real time spin fluctuation for  $i$ th site. The initial distribution  $C_{S_z}(i, t = 0)$  is also a Kronecker delta function, and the spatiotemporal distribution  $C_{S_z}(i, t)$  describes the spreading of the spin fluctuation across the spin chain.

The asymptotic time behavior of correlation functions  $C_E(i, t)$  or  $C_{S_z}(i, t)$  can give the information of the transport behavior for corresponding quantities of energy or the  $z$  component of spin. If the asymptotic correlation function approaches the Gaussian normal distribution as

$$\rho_G(i, t) = \frac{1}{\sqrt{4\pi Dt}} e^{-\frac{i^2}{4Dt}}, \quad (6)$$

which is a discrete solution of standard diffusion equation  $\partial \rho / \partial t = D \partial^2 \rho / \partial x^2$  with initial condition  $\rho(x, t = 0) = \delta(x)$ , then it can be concluded that the diffusion behavior for the corresponding quantity is normal and the constant  $D$  is the diffusion constant for that quantity.

As a result, the corresponding MSD  $\langle \Delta x^2(t) \rangle$  defined as

$$\langle \Delta x^2(t) \rangle = \sum_i i^2 C(i, t) \quad (7)$$

will follow a linear time dependence for normal diffusion as

$$\langle \Delta x^2(t) \rangle = \sum_i i^2 \rho_G(i, t) = 2Dt. \quad (8)$$

If the diffusion behavior is not normal, the asymptotic MSD usually follows a power-law time dependence as

$$\langle \Delta x^2(t) \rangle \propto t^\beta. \quad (9)$$

The exponent  $\beta = 2$  describes the ballistic diffusion, and  $1 < \beta < 2$  represents a superdiffusion behavior.

In the numerical simulations, the fourth-order Runge-Kutta integration method is applied with a small time step  $h = 0.01$ . The initial setup for  $\{\tilde{S}_i\}$  is chosen to ensure a specified energy density  $e$ , and the corresponding temperature  $T$  can be resolved from Eq. (3). After a transient time of  $5 \times 10^5$ , another longer time of  $5 \times 10^6$  will be performed to record the data. In order to have better accuracy of the correlation functions, 50 runs with random initial conditions for a same energy density  $e$  will be simulated mimicking the ensemble average. The effective result is equivalent to the result of a single run with a total recording time of  $2.5 \times 10^8$ .

### III. ENERGY DIFFUSION

We first study the diffusion behavior for energy at different temperatures. It is well known that the nonlinear classical Heisenberg spin chain can be approximated into a linearized spin model with collective motions described by spin waves in the low-temperature limit  $T \rightarrow 0$ .

For a linear system without interaction between different normal modes, the energy diffusion behavior should be ballistic due to the infinite long mean-free path for energy carriers. Therefore in the low-temperature regime, the transient diffusion behavior should be close to ballistic for a chain with finite length.

For low temperature  $T \approx 0.1$  with the energy density set as  $e = -0.9$ , the energy distributions  $C_E(i, t)$  at three different correlation times  $t = 50, 100$ , and  $150$  are plotted in Fig. 2 with chain length  $N = 701$ . From upper to lower in the central position, the energy distributions  $C_E(i, t)$  are plotted as solid black ( $t = 50$ ), red ( $t = 100$ ), and blue ( $t = 150$ ) lines. It can be seen that there are two wave fronts for each  $C_E(i, t)$  moving outwards with a constant velocity around 1. This is a typical signature for ballistic diffusion. It is consistent with the expectation that the nonlinear inaction between different modes of spin waves is very small at such a low-temperature situation, and an almost ballistic diffusion behavior should appear for short correlation times as the chain length is finite.

However, if the temperature is increased to  $T \approx 0.75$  with the energy density set as  $e = -0.4$ , the normal diffusion behavior for energy can be obtained for the finite chain size  $N = 701$ . In Fig. 3(a) the energy distributions  $C_E(i, t)$  at temperature  $T \approx 0.75$  are plotted for three different correlation times  $t = 400, 700$ , and  $1000$ . Comparing with those energy distributions at  $T \approx 0.1$  (in Fig. 2), it can be seen that the constantly moving wave fronts of  $C_E(i, t)$  disappear here for

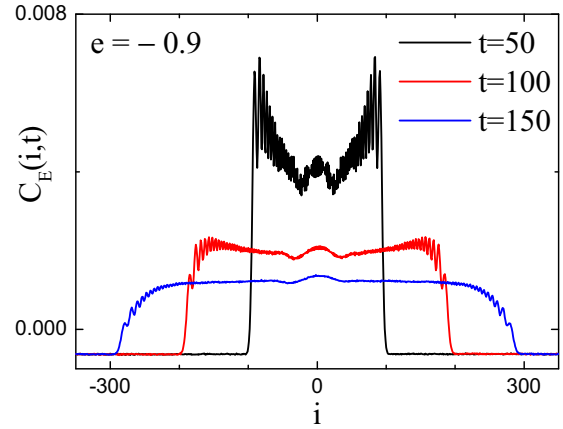


FIG. 2. Energy distribution  $C_E(i, t)$  for the 1D isotropic Heisenberg spin chain with the energy density  $e = -0.9$  and the corresponding temperature  $T \approx 0.1$ . The distributions at three different correlation times  $t = 50, 100$ , and  $150$  are plotted as solid black, red, and blue lines (from upper to lower in central position). The energy diffusion exhibits an almost ballistic behavior as the fronts of distributions  $C_E(i, t)$  travel towards outside with a constant velocity close to 1. The chain size is set as  $N = 701$ .

$T \approx 0.75$ . The height of the bell shape  $C_E(i, t)$  decreases as the correlation time increases, which is a signature of diffusive behavior.

In order to determine the actual diffusion behavior, we plot the rescaled energy distributions  $t^{1/2} C_E(i, t)$  as the function

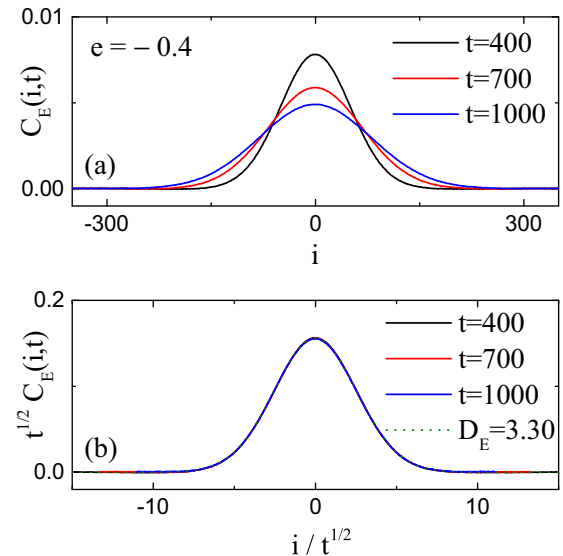


FIG. 3. Energy distribution  $C_E(i, t)$  for the 1D isotropic Heisenberg spin chain with the energy density  $e = -0.4$  and the corresponding temperature  $T \approx 0.75$ . (a) The distributions  $C_E(i, t)$  at three different correlation times  $t = 400, 700$ , and  $1000$  are plotted as solid black, red, and blue lines (from upper to lower in central position). (b) The rescaled distributions  $t^{1/2} C_E(i, t)$  as the function of rescaled position  $i/t^{1/2}$ . All three rescaled distributions collapse into one single curve which can be fitted perfectly by a Gaussian distribution of Eq. (6) with diffusion constant  $D_E = 3.30$ . The chain size is set as  $N = 701$ .

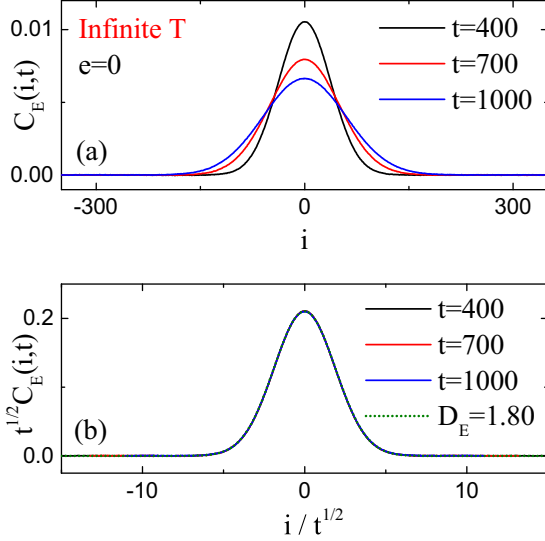


FIG. 4. Energy distribution  $C_E(i, t)$  for the 1D isotropic Heisenberg spin chain with the energy density  $e = 0$  and the corresponding temperature  $T = \infty$ . (a) The distributions  $C_E(i, t)$  at three different correlation times  $t = 400, 700$ , and  $1000$  are plotted as solid black, red, and blue lines (from upper to lower in central position). (b) The rescaled distributions  $t^{1/2}C_E(i, t)$  as the function of rescaled position  $i/t^{1/2}$ . All three rescaled distributions collapse into one single curve which can be fitted perfectly by a Gaussian distribution of Eq. (6) with diffusion constant  $D_E = 1.80$ . The chain size is set as  $N = 701$ .

of rescaled chain position  $i/t^{1/2}$  in Fig. 3(b). It can be seen that all three rescaled energy distributions  $t^{1/2}C_E(i, t)$  at correlation times  $t = 400, 700$ , and  $1000$  collapse into one single curve. This single curve can be well fitted by the Gaussian distribution of Eq. (6) with the fitted diffusion constant  $D_E = 3.30$ . Therefore, the normal energy diffusion can be confirmed for the classical Heisenberg spin chain at temperature  $T \approx 0.75$  even for a finite chain with  $N = 701$ .

In Fig. 4 the energy distributions  $C_E(i, t)$  at infinite temperature  $T = \infty$  with energy density  $e = 0$  are plotted. The  $C_E(i, t)$  at three different correlation times are plotted as solid black ( $t = 400$ ), red ( $t = 700$ ), and blue ( $t = 1000$ ) lines in Fig. 4(a). A similar diffusive behavior as that for  $T \approx 0.75$  is clearly seen. To determine the actual diffusion behavior, the rescaled energy distributions  $t^{1/2}C_E(i, t)$  as the function of rescaled chain position  $i/t^{1/2}$  are plotted in Fig. 4(b). It is found that all the rescaled energy distributions  $t^{1/2}C_E(i, t)$  at three different correlation times  $t = 400, 700$ , and  $1000$  collapse into one single curve which can be well fitted by a Gaussian distribution of Eq. (6) with the fitted diffusion constant  $D_E = 1.80$ . The normal energy diffusion behavior is also confirmed for the 1D classical Heisenberg spin chain at infinite temperature. The diffusion constant  $D_E = 1.80$  at infinite temperature  $T = \infty$  is smaller than the diffusion constant  $D_E = 3.30$  at finite temperature  $T \approx 0.75$ .

The reason that we cannot observe normal energy diffusion for the classical Heisenberg spin chain at a low-temperature regime is because the chain size of  $N = 701$  we used is not long enough. Since the mean-free path for energy carriers is diverging in the low-temperature limit corresponding to linear system, the chain size needed to observe asymptotic normal

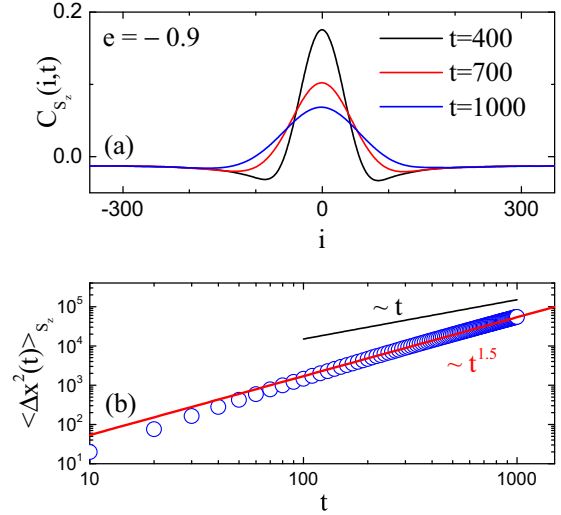


FIG. 5. Spin distribution  $C_{S_z}(i, t)$  for the 1D isotropic Heisenberg spin chain with the energy density  $e = -0.9$  and the corresponding temperature  $T \approx 0.1$ . (a) The distributions  $C_{S_z}(i, t)$  at three different correlation times  $t = 400, 700$ , and  $1000$  are plotted as solid black, red, and blue lines (from upper to lower in central position). (b) The MSD  $\langle \Delta x^2(t) \rangle_{S_z}$  as the function of correlation time  $t$ . The hollow circles are numerical data, and the red solid line through the circles is proportional to  $t^{1.5}$ . The black solid line above the circles proportional to  $t$  is plotted for comparison. The spin diffusion at this temperature is superdiffusion at least for the chain size  $N = 701$ .

energy diffusion should also diverge, which is out of our computation ability. However, for a temperature larger than  $T = 0.75$ , the asymptotic normal energy diffusion behavior can already be confirmed even for a chain size of  $N = 701$ . We should point out that  $T \approx 0.75$  is not a critical value separating normal and anomalous diffusion as it might be smaller or even vanish in the thermodynamic limit  $N \rightarrow \infty$ .

#### IV. SPIN DIFFUSION

For the isotropic 1D classical Heisenberg spin chain, the total spin  $\vec{S} = \sum_i \vec{S}_i$  and its three components are conserved. Since the three components are symmetric, we can only consider the diffusion process for the  $z$  component of the total spin  $S_z = \sum_i S_{i,z}$ .

We first consider the spin diffusion in the low-temperature region. In Fig. 5(a) the spatiotemporal distributions  $C_{S_z}(i, t)$  are plotted at low temperature  $T \approx 0.1$  with energy density set as  $e = -0.9$ . The distributions  $C_{S_z}(i, t)$  at three different correlation times  $t = 400, 700$ , and  $1000$  are plotted as solid black, red, and blue lines (from upper to lower in central position). Although the distributions  $C_{S_z}(i, t)$  without moving fronts look like diffusive ones, they are actually not a Gaussian distribution. The background values for  $C_{S_z}(i, t)$  are negative even after the adding of the extra term  $1/(N-1)$  in Eq. (5). To determine whether the diffusion is Gaussian or not, the time dependence of the MSD  $\langle \Delta x^2(t) \rangle_{S_z}$  needs to be considered.

In Fig. 5(b) the MSD  $\langle \Delta x^2(t) \rangle_{S_z}$  is plotted as the function of correlation time  $t$ . It can be seen that the time dependence of  $\langle \Delta x^2(t) \rangle_{S_z}$  can be better fitted as  $\langle \Delta x^2(t) \rangle_{S_z} \propto t^\beta$  with  $\beta = 1.50$ . This time dependence is faster than linear

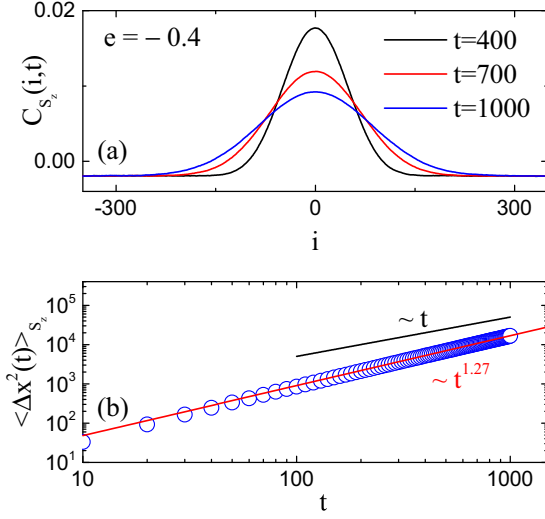


FIG. 6. Spin distribution  $C_{S_z}(i, t)$  for the 1D isotropic Heisenberg spin chain with the energy density  $e = -0.4$  and the corresponding temperature  $T \approx 0.75$ . (a) The distributions  $C_{S_z}(i, t)$  at three different correlation times  $t = 400, 700,$  and  $1000$  are plotted as solid black, red, and blue lines (from upper to lower in central position). (b) The MSD  $\langle \Delta x^2(t) \rangle_{S_z}$  as the function of correlation time  $t$ . The hollow circles are numerical data, and the red solid line through the circles is proportional to  $t^{1.27}$ . The black solid line above the circles proportional to  $t$  is plotted for comparison. The spin diffusion at this temperature is also superdiffusive at least for the chain size  $N = 701$ .

time dependence, and the spin diffusion at low temperature  $T \approx 0.1$  is superdiffusive at least for the chain size  $N = 701$  studied here.

We next consider the spin diffusion at temperature of  $T \approx 0.75$  with energy density  $e = -0.4$ . At this temperature, the normal energy diffusion is already obtained. In Fig. 6(a) the spin distributions  $C_{S_z}(i, t)$  at three different correlation times  $t = 400, 700,$  and  $1000$  are plotted as solid black, red, and blue lines (from upper to lower in central position). The negative background values for  $C_{S_z}(i, t)$  remind us the diffusion behavior is still not normal.

In Fig. 6(b) the MSD  $\langle \Delta x^2(t) \rangle_{S_z}$  is plotted as the function of correlation time  $t$ . It can be seen that the numerical data can be better fitted by a power-law dependence as  $\langle \Delta x^2(t) \rangle_{S_z} \propto t^\beta$  with  $\beta = 1.27$ . The spin diffusion at this temperature is still a superdiffusive behavior. The exponent  $\beta = 1.27$  here at  $T \approx 0.75$  is smaller than that of  $\beta = 1.50$  at  $T \approx 0.1$ .

At the infinite temperature  $T = \infty$  with energy density set as  $e = 0$ , the spin distributions  $C_{S_z}(i, t)$  are plotted in Fig. 7(a) for a chain with  $N = 1501$ . The  $C_{S_z}(i, t)$  at three different correlation times  $t = 1200, 2100,$  and  $3000$  are plotted as solid black, red, and blue lines (from upper to lower in central position). The background values for  $C_{S_z}(i, t)$  are now vanishing, which is different from that at finite temperatures.

In Fig. 7(b) the rescaled spin distributions  $t^{1/2}C_{S_z}(i, t)$  are plotted as the function of rescaled positions  $i/t^{1/2}$ . All three rescaled distributions  $t^{1/2}C_{S_z}(i, t)$  at correlation times  $t = 1200, 2100,$  and  $3000$  collapse into one single curve, and this curve can be well fitted by the Gaussian distribution

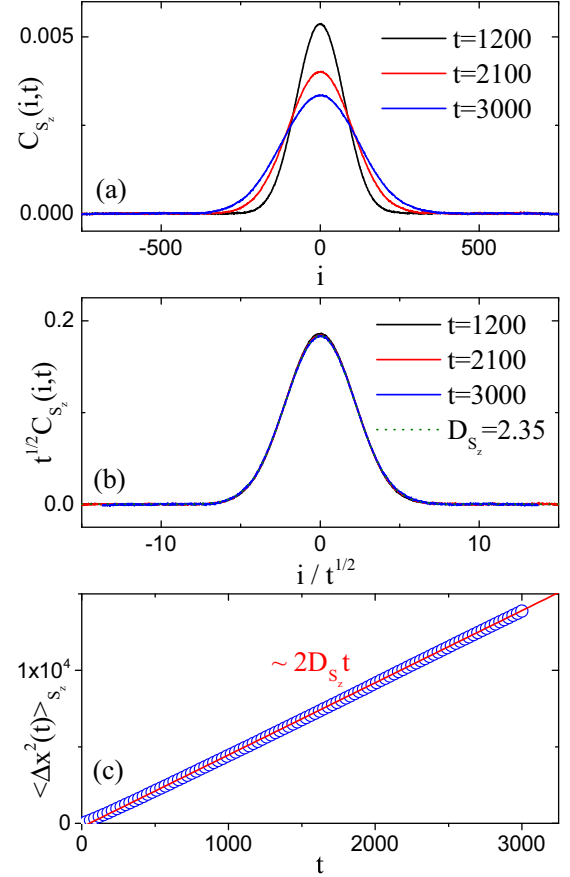


FIG. 7. Spin distribution  $C_{S_z}(i, t)$  for the 1D isotropic Heisenberg spin chain with the energy density  $e = 0$  and the corresponding temperature  $T = \infty$ . (a) The distributions  $C_{S_z}(i, t)$  at three different correlation times  $t = 1200, 2100,$  and  $3000$  are plotted as solid black, red, and blue lines (from upper to lower in central position). (b) The rescaled distributions  $t^{1/2}C_{S_z}(i, t)$  as the function of rescaled position  $i/t^{1/2}$ . All three rescaled distributions collapse into one single curve which can be fitted very well by a Gaussian distribution of Eq. (6) with diffusion constant  $D_{S_z} = 2.35$ . (c) The MSD  $\langle \Delta x^2(t) \rangle_{S_z}$  as the function of correlation time with a linear-linear plot. The straight line is  $\langle \Delta x^2(t) \rangle_{S_z} = -250 + 2D_{S_z}t$  fits well with the numerical data demonstrating a normal diffusion behavior. The chain size is set as  $N = 1501$ .

of Eq. (6) with the diffusion constant  $D_{S_z} = 2.35$ . Therefore at the infinite temperature, the normal spin diffusion is also observed for a finite chain size  $N = 1501$ .

For spin diffusion, it is hard to give a conclusion for finite temperatures as the chain length we used is far from thermodynamical limit. But for the infinite temperature case, the normal spin diffusion behavior obeying the conventional spin-diffusion theory can be assured with much confidence. The actual spin diffusion behavior at a low temperature needs more careful treatment with more powerful numerical simulations.

## V. CONCLUSION

We have systematically investigated the energy and spin diffusions for the 1D classical and isotropic Heisenberg spin

chain. The energy and spin distributions are calculated for a finite spin chain with size up to  $N = 1501$ . For energy diffusion, the normal diffusion behavior can be obtained for a temperature higher than  $T \approx 0.75$ . For spin diffusion at finite temperature, the diffusion behavior can be describe by a superdiffusion with power-law time dependence  $\langle \Delta x^2(t) \rangle_{S_z} \propto t^\beta$  and the exponent  $\beta$  is larger than 1. The exponent  $\beta$  decreases as the temperature increases. At infinite temperature, the normal diffusion behavior obeying the conven-

tional spin-diffusion theory is also obtained for the spin diffusion.

#### ACKNOWLEDGMENTS

This work is supported by National Natural Science Foundation of China with Grant No. 11775158, the Science and Technology Commission of Shanghai Municipality with Grant No. 17ZR1432600, and the Scientific Research Funds of Huaqiao University.

- 
- [1] N. Bloembergen, *Phys. (Utrecht)* **15**, 386 (1949).
  - [2] L. van Hove, *Phys. Rev.* **95**, 1374 (1954).
  - [3] G. Muller, *Phys. Rev. Lett.* **60**, 2785 (1988).
  - [4] R. W. Gerling and D. P. Landau, *Phys. Rev. B* **42**, 8214 (1990).
  - [5] J. Liu, N. Srivastava, V. S. Viswanath, and G. Muller, *J. Appl. Phys.* **70**, 6181 (1991).
  - [6] O. F. de Alcantara Bonfim, and G. Reiter, *Phys. Rev. Lett.* **69**, 367 (1992).
  - [7] M. Bohm, R. W. Gerling, and H. Leschke, *Phys. Rev. Lett.* **70**, 248 (1993).
  - [8] S. W. Lovesey and E. Balcar, *J. Phys.: Condens. Matter* **6**, 1253 (1994).
  - [9] N. Srivastava, J. Liu, V. S. Viswanath, and G. Muller, *J. Appl. Phys.* **75**, 6751 (1994).
  - [10] D. Bagchi, *Phys. Rev. B* **87**, 075133 (2013).
  - [11] V. Constantoudis and N. Theodorakopoulos, *Phys. Rev. E* **55**, 7612 (1997).
  - [12] S. Lepri, R. Livi, and A. Politi, *Phys. Rev. Lett.* **78**, 1896 (1997).
  - [13] S. Lepri, R. Livi, and A. Politi, *Phys. Rep.* **377**, 1 (2003).
  - [14] A. Dhar, *Adv. Phys.* **57**, 457 (2008).
  - [15] S. Liu, X. F. Xu, R. G. Xie, G. Zhang, and B. Li, *Eur. Phys. J. B* **85**, 337 (2013).
  - [16] B. Hu, B. Li, and H. Zhao, *Phys. Rev. E* **57**, 2992 (1998).
  - [17] B. Hu, B. Li, and H. Zhao, *Phys. Rev. E* **61**, 3828 (2000).
  - [18] K. Aoki and D. Kusnezov, *Phys. Lett. A* **265**, 250 (2000).
  - [19] C. Giardinà, R. Livi, A. Politi, and M. Vassalli, *Phys. Rev. Lett.* **84**, 2144 (2000).
  - [20] O. V. Gendelman and A. V. Savin, *Phys. Rev. Lett.* **84**, 2381 (2000).
  - [21] O. Narayan and S. Ramaswamy, *Phys. Rev. Lett.* **89**, 200601 (2002).
  - [22] S. Denisov, J. Klafter, and M. Urbakh, *Phys. Rev. Lett.* **91**, 194301 (2003).
  - [23] N. Li, B. Li, and S. Flach, *Phys. Rev. Lett.* **105**, 054102 (2010).
  - [24] L. Wang and T. Wang, *Europhys. Lett.* **93**, 54002 (2011).
  - [25] L. Wang, B. Hu, and B. Li, *Phys. Rev. E* **86**, 040101(R) (2012).
  - [26] Y. Zhong, Y. Zhang, J. Wang, and H. Zhao, *Phys. Rev. E* **85**, 060102(R) (2012).
  - [27] L. Wang, B. Hu, and B. Li, *Phys. Rev. E* **88**, 052112 (2013).
  - [28] S. G. Das, A. Dhar, and O. Narayan, *J. Stat. Phys.* **154**, 204 (2014).
  - [29] A. V. Savin and Y. A. Kosevich, *Phys. Rev. E* **89**, 032102 (2014).
  - [30] L. Wang, L. Xu, and H. Zhao, *Phys. Rev. E* **91**, 012110 (2015).
  - [31] S. Chen, Y. Zhang, J. Wang, and H. Zhao, *J. Stat. Mech.* (2016) 033205.
  - [32] L. Xu and L. Wang, *Phys. Rev. E* **96**, 052139 (2017).
  - [33] C. W. Chang, D. Okawa, H. Garcia, A. Majumdar, and A. Zettl, *Phys. Rev. Lett.* **101**, 075903 (2008).
  - [34] V. Lee, C. H. Wu, Z. X. Lou, W. L. Lee, and C. W. Chang, *Phys. Rev. Lett.* **118**, 135901 (2017).
  - [35] X. Xu, L. F. C. Pereira, Y. Wang, J. Wu, K. Zhang, X. Zhao, S. Bae, C. T. Bui, R. Xie, J. T. L. Thong, B. H. Hong, K. P. Loh, D. Donadio, B. Li, and B. Ozyilmaz, *Nat. Commun.* **5**, 3689 (2014).
  - [36] A. V. Savin, G. P. Tsironis, and X. Zotos, *Phys. Rev. B* **72**, 140402(R) (2005).
  - [37] H. Zhao, *Phys. Rev. Lett.* **96**, 140602 (2006).
  - [38] S. Liu, P. Hänggi, N. Li, J. Ren, and B. Li, *Phys. Rev. Lett.* **112**, 040601 (2014).
  - [39] Y. Li, S. Liu, N. Li, P. Hänggi, and B. Li, *New J. Phys.* **17**, 043064 (2015).
  - [40] M. E. Fisher, *Am. J. Phys.* **32**, 343 (1964).